J. Fluid Mech. (1984), *vol.* 141, *pp.* 347–364
Printed in Great Britain

Progress towards a theory of jet-flap thrust recovery

By P. M. BEVILAQUA, E. F. SCHUM AND C. J. WOAN
Rockwell International, North American Aircraft Operations, Columbus, Ohio

(Received 28 February 1983 and in revised form 31 October 1983)

A combination of analysis and testing has been utilized to develop a theory of jet-flap thrust recovery at the low speeds and high deflection angles characteristic of V/STOL lift systems. The contribution of jet mixing to the loss of thrust recovery has been computed with a viscid/inviscid interaction analysis. The results of this computation are compared to surface pressure and wake survey measurements made with a two-dimensional jet-flapped airfoil model. It is concluded that the jet-mixing drag causes a small loss of recovery at small values of the jet-thrust coefficient and deflection angle. However, at larger values of either jet parameter, the mainstream separates from the airfoil, producing a large loss of recovery. The loss increases suddenly, since it is due to bursting of the leading-edge separation bubble.

1. Introduction

A jet sheet directed down from the trailing edge of a wing, as shown in figure 1, increases the wing lift, not only as a reaction to the jet thrust, but also as a result of changes induced in the wing surface-pressure distribution by the deflection of the mainstream. This phenomenon is called the jet-flap effect by analogy to the action of a mechanical flap. It makes some contribution to the forces induced by all V/STOL lift systems. However, besides inducing wing lift, the jet flap also induces a thrust greater than the horizontal component of the jet reaction force. This was discovered during testing of jet-flapped airfoils at the British National Gas Turbine Establishment (Davidson 1956). As a result of this discovery, Stratford (1956*a*) postulated that, in ideal flow, the total jet thrust would always be 'recovered' as a horizontal force, regardless of the initial deflection angle, because the jet is ultimately turned in the direction of the freestream.

This hypothesis was received with considerable scepticism, since it implies that the jet thrust acts in two directions at the same time; but the existence of the thrust-recovery phenomenon was confirmed in tests performed by Stratford (1956*b*), Williams, Butler & Wood (1961) and Foley (1962). However, only partial recovery was measured at all jet-deflection angles, with a significant loss of thrust as the deflection angle was increased beyond 60°. This loss has been attributed to various real-fluid effects: Stratford (1956*c*) argued that the jet entrainment induces a pressure drag on the wing, and Wygnanski (1966) suggested that this jet drag increases with the jet-deflection angle. On the other hand, Williams *et al.* (1961) pointed out that separation of the flow over the airfoil would also cause a loss of thrust, while Tsongas (1962) argued that separation of the freestream from the jet flap itself causes the thrust loss. Thus, although the existence of thrust recovery has been shown, the real-fluid effects that reduce it are incompletely understood. Consequently, there is no theory for predicting the net thrust of a jet flap.

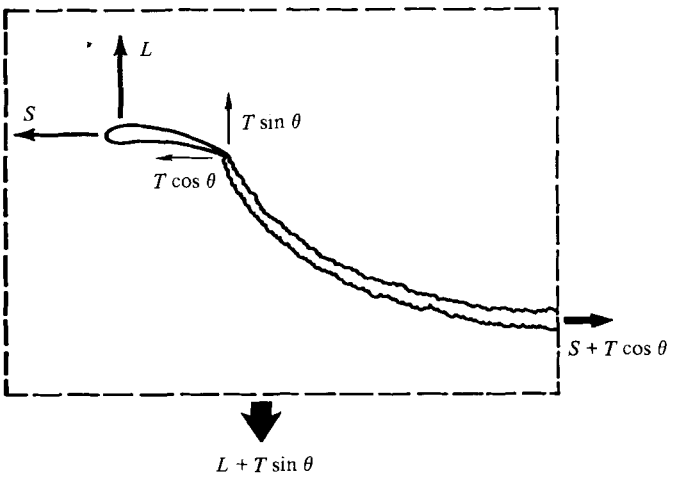

FIGURE 1. Control volume showing the forces on the airfoil and nozzle: T, jet thrust; L, aerodynamic lift; S, leading-edge suction.

Spence's (1956) now-classical jet-flap theory, in which the inertia of the jet sheet is balanced by a pressure difference across the jet, is used for calculating lift under the assumption that the thrust of the jet is constant, while an empirical factor is used to specify a loss of thrust for calculating drag (McCormick 1967). Such empirical factors are valid only for small variations from the original data base. Thrust-recovery data are available for a complete range of deflection angles, but only for jet-thrust coefficients less than unity. Since the thrust coefficient is much greater than unity during takeoff and landing, there are actually no data for specifying the thrust recovery of V/STOL propulsion systems.

More recently, Wilson (1973) used an empirical sink distribution on the jet axis to show that the computed pressure drag on the airfoil is on the order of the thrust loss measured at small deflection angles. However, this approach may not be valid for V/STOL predictions, since it is not known if the loss of thrust at large deflection angles is due to the jet mixing drag. Further, sink distributions model just half of the jet/airfoil interaction: the pressure drag induced on the airfoil. The equal but opposite loss of jet thrust is neglected. When the thrust loss is large, the jet path and therefore the airfoil lift are changed. Thus a complete theory must include the variation of the jet thrust.

The purpose of this paper is to describe progress in developing a theory of jet-flap thrust recovery at the large thrust coefficients and deflection angles characteristic of V/STOL lift systems. A combination of analysis and testing has been utilized. In §2 the inviscid mechanism of thrust recovery and the way in which viscosity reduces the jet thrust are discussed. A viscid/inviscid interaction analysis developed to compute the jet drag is presented in §3. The experimental apparatus and test procedures used to measure the thrust recovery are described in §4. In §5 the analytical results are compared to measured surface pressure and wake survey data. It is concluded, in §6, that the large loss of thrust at large jet-deflection angles is due to bursting of the airfoil leading-edge separation bubble, and not jet entrainment drag.

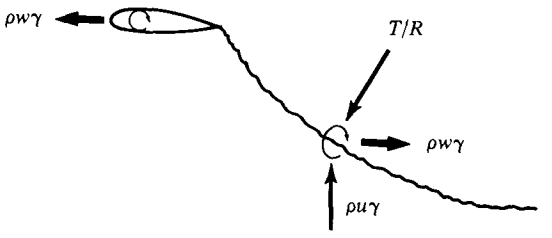

FIGURE 2. The mutually induced forces on bound vortices in the wing and jet sheet.

2. Jet-flap theory

2.1. *Thrust-recovery mechanism*

The mechanism of thrust recovery can be explained in terms of equal but opposite pressure forces which act on the airfoil and jet sheet. These forces originate in an inviscid interaction between the airfoil circulation and the vorticity associated with the jet sheet. According to Spence's (1956) theory, the pressure force which balances the jet inertia can be represented by the force on an equivalent vortex sheet located along the jet axis; that is, $\Delta P = \rho u \gamma$. Thus γ_j, the vorticity in a section of the jet sheet, induces an upwash velocity at a vortex segment bound in the wing, as shown in figure 2. This produces a thrust on the wing of magnitude $\rho\gamma_w\gamma_j/2\pi r$. Similarly, γ_w, the wing vortex, induces a downwash at the jet vortex, which then experiences an equal but opposite force of magnitude $\rho\gamma_j\gamma_w/2\pi r$. The integrated effect of all such vortex interactions produces the thrust recovery.

The total thrust of the jet at downstream infinity is the sum of the horizontal component of the initial reaction force and the net vortex force. If it is assumed that both the jet and freestream are inviscid, the only force on the jet is due to the pressure difference across it. The horizontal component of this force is

$$\Sigma\rho w\gamma = -\int_0^\infty \mathrm{d}P \sin\theta \,\mathrm{d}s, \tag{1}$$

in which w is the net downwash velocity, θ is the local jet-deflection angle, and $\mathrm{d}s = R\,\mathrm{d}\theta$ is the jet arclength. The pressure difference is balanced by the inertia due to jet curvature, $\mathrm{d}P = T/R$. The jet thrust is constant because the flow expands isentropically. Thus integration yields, for the horizontal force on the jet,

$$\Sigma\rho w\gamma = T(1-\cos\theta_0), \tag{2}$$

where θ_0 is the initial deflection angle. The thrust component of the initial jet reaction force is $T\cos\theta_0$, and so the total thrust of the jet is recovered as a horizontal force. Similarly, the thrust on the airfoil is the sum of the initial force on the nozzle, $T\cos\theta_0$, plus the pressure thrust induced on the airfoil, $T(1-\cos\theta_0)$.

There is still some confusion in the literature regarding the mechanism of thrust recovery. As part of a series of experiments at Stanford University, Quanbeck (1963) integrated the surface-pressure distribution of a jet-flapped airfoil as the jet-deflection angle was varied. Because the horizontal component of the surface-pressure integral did not vary, it was concluded that the entire jet thrust was recovered as a force on the nozzle. However, in these tests the jet was deflected by utilizing the Coanda effect (see Metral & Zerner 1948) to turn it over a short flap. Unless there is a large loss of thrust, the pressure force initially required to deflect the jet over the flap is the

same as the force required to turn it back in the direction of the freestream. Therefore the thrust induced on the leading edge of the airfoil would always equal the flap drag due to the Coanda effect, and the net pressure integral would not vary. Today it is no longer doubted that the jet thrust is recovered on the airfoil surface, primarily as a leading-edge suction.

2.2. *Thrust-loss mechanisms*

Real-fluid effects can reduce the thrust recovery through two separate mechanisms. The jet flap induces a very large suction peak near the leading edge of the airfoil. If the boundary layer separates in this region, the resulting loss of suction reduces the thrust recovery. This loss becomes more likely as the jet-thrust coefficient and deflection angle are increased.

The thrust recovery may also be reduced by the mixing of the jet and freestream due to viscosity. This loss is not the result of friction drag between the jet and freestream; rather it is due to equal but opposite pressure forces induced on the airfoil and jet. Entrainment by the jet accelerates the flow over the after surfaces of the airfoil, and thus changes the base pressure. The mechanism of the corresponding change in jet thrust may not be as apparent. This reaction force is conceptually similar to the drag experienced by a sink in an external stream. However, the sink drag is only an irrotational simulation of the jet mechanism. The fluid entrained into the jet becomes rotational, so that understanding how the reaction force actually develops requires consideration of the jet mixing process.

This process is basically an inelastic collision between the jet and surrounding fluid. As such, jet mixing is governed by the same laws of momentum and energy conservation as simple collisions between discrete particles. If the mixing occurs in a region of constant static pressure, the thrust of the jet is conserved. But, if the jet passes through a region where the static pressure P_* is different from the undisturbed pressure P_∞ at infinity, the mixing changes the momentum flux. The following simple analysis illustrates this phenomenon.

Inside the region where the pressure is P_*, the velocities in the jet and coflowing stream, before mixing, are assumed to be

$$U_j^* = \left[\frac{2(P_0 - P_*)}{\rho}\right]^{\frac{1}{2}}, \tag{3}$$

$$U_s^* = \left[U_\infty^2 + \frac{2(P_0 - P_*)}{\rho}\right]^{\frac{1}{2}}, \tag{4}$$

in which P_0 is the stagnation pressure of the jet and U_∞ is the velocity of the coflowing stream at infinity. Momentum is conserved during the mixing process itself, so that

$$\dot{m}_j U_j^* + \dot{m}_s U_s^* = (\dot{m}_j + \dot{m}_s) U_m^*, \tag{5}$$

in which $\dot{m}_j$ is the initial mass flux of the jet, $\dot{m}_s$ is the quantity of mass entrained by the jet, and U_m^* is the average velocity of the mixed flow.

The velocity of the mixed stream changes as it passes into the region of undisturbed pressures; the velocity becomes

$$U_m = \left[U_m^{*2} - \frac{2(P_\infty - P_*)}{\rho}\right]^{\frac{1}{2}}. \tag{6}$$

The ratio of the final thrust of the mixed stream $(\dot{m}_p + \dot{m}_s) U_m$ to the thrust $\dot{m}_p U_j$ obtained by an isentropic expansion of the jet, without mixing, to the final pressure

may be evaluated by substituting in turn for U_m, then U_m^*, and finally for U_j^* and U_s^*. Performing these substitutions yields for this ratio

$$\phi = [1+2M[(1+H)^{\frac{1}{2}}(U^2+H)^{\frac{1}{2}}-H]+M^2U^2]^{\frac{1}{2}}-MU, \tag{7}$$

in which $M = \dot{m}_s/\dot{m}_p$ is the entrainment ratio, $U = U_\infty/U_j$ is the velocity ratio, and $H = 2(P_\infty - P_*)/\rho U_j^2$ is the normalized pressure change.

If there is no pressure difference then $H = 0$ and the solution reduces to that for free jet mixing; that is, $\phi = 1$. Similarly, if there is no mixing between the jet and coflowing stream, then $M = 0$ and the thrust is conserved in this case also. However, if the pressure in the mixing region is higher than the ambient pressure, the thrust of the jet is reduced. For the case in which $U_s = 0$, the thrust ratio has the simple form

$$\phi = 1-MU, \tag{8}$$

and it is seen that the jet thrust decreases with increasing entrainment. Because there is a region of increased static pressure behind the trailing edge of the jet-flapped airfoil, entrainment reduces the jet thrust. According to Newton's law of action and reaction, the loss of jet thrust due to mixing must be equal to the pressure drag that the mixing induces on the wing.

Interestingly, if the pressure in the mixing region is below the ambient pressure, then the thrust of the jet is actually increased. For the case in which $U_\infty = 0$, the thrust ratio also has a simple form,

$$\phi = (1+M)^{\frac{1}{2}}, \tag{9}$$

and jet thrust increases with increasing entrainment. Stratford (1956*b*) attempted to utilize this phenomenon to reduce the thrust loss, but concluded that the effect is small.

In order to determine the relative importance of separation and jet-mixing drag in reducing the thrust recovery, the jet drag will be computed for unseparated flow and compared with the drag actually obtained on a wind tunnel model under the same conditions. Differences between these cases will be studied to identify the loss mechanisms. In §3 the method of calculating the jet drag will be developed from the principles outlined here.

3. Analytical method

In principle, the thrust recovery could be predicted by a solution of the Reynolds-averaged Navier–Stokes equation for the entire flow field. However, the number of parameters that characterize the flow, the number of grid points required to capture the details of the solution, and the nonlinear nature of the equations themselves would make this a formidable task, even on the next generation of computers. Thus the basis of our analysis is a separation of the flow field into two regions: the region of turbulent mixing within the jet, and the inviscid region surrounding it. The thrust recovery is computed by matching a viscous analysis of the turbulent jet to an inviscid analysis of the jet flap. This solution procedure will be described in the following paragraphs.

3.1. *Viscous jet analysis*

A finite-difference analysis utilizing a two-equation turbulence kinetic energy model was developed to predict the jet entrainment and thrust loss. Since there is a primary direction of flow (along the jet), streamwise diffusion and upstream convection can be neglected. This reduces the governing elliptic equations to a parabolic set which

can be solved by marching along the jet in the streamwise direction. The effect of the radial pressure gradient on the mean flow was neglected. But since the increase in the jet mixing rate due to curvature is central to Wygnanski's (1966) jet-drag hypothesis, its effect on the turbulence was modelled. Hunt & Joubert (1979) argued that the effect of curvature is to transfer energy from the streamwise component of the turbulence to the transverse component. They suggested adding a term to the turbulent energy and dissipation equations to simulate this process. We have used their form of the turbulence equations.

The governing equations for the conservation of mass and momentum, as well as the equations for the turbulence energy and dissipation, were solved using the basic scheme devised by Patankar & Spalding (1970). All the equations may be written in the general form

$$\rho u \frac{\partial \xi}{\partial s} = \frac{\partial}{\partial s}\left(\mu \frac{\partial \xi}{\partial s}\right) + S, \tag{10}$$

in which the general dependent variable ξ represents any of the mean-flow or turbulence variables, while μ and S represents the corresponding diffusion and production terms, and s is the streamwise coordinate. All of the constants in the turbulence equation were given the values suggested by Launder & Spalding (1972). This set of equations is solved using a semi-implicit line-by-line procedure in the streamwise direction, and the tridiagonal-matrix algorithm in the transverse direction, with variable under-relaxation. A complete description of this jet analysis is given by Bevilaqua, Cole & Schum (1980).

3.2. *Inviscid jet-flap analysis*

A higher-order panel method was used to predict the jet trajectory. The basic mathematical problem to be solved requires finding a velocity potential that is harmonic and satisfies the boundary conditions of uniform flow at infinity and flow tangent to the surface of the airfoil and centreline of the jet. Since the shape of the jet is initially unknown, the inertial force in the jet was related to the strength of the vortex sheet bound in the jet

$$\rho u \gamma = \frac{T}{R}, \tag{11}$$

according to the jet-flap theory of Spence (1956). This provides an additional, dynamic boundary condition.

The inviscid solution is obtained using the parabolic-panel method due to Hess (1973), and employs Halsey's (1974) jet iteration scheme to determine the jet shape. The airfoil and jet sheet were represented by the panel distribution shown in figure 3. The singularity strengths vary linearly with respect to the local panel chord.

The streamwise variation of the jet thrust and the sinks which represent the jet entrainment are considered to be known from the turbulent-jet analysis. The unknown vortex strengths on the airfoil and jet boundaries are determined by satisfying the kinematic boundary condition on the airfoil, the dynamic boundary condition on the jet, and the condition that the jet vortex strength goes to zero at downstream infinity. The jet position is then updated such that the kinematic boundary condition is satisfied at all the jet control points; the solution for the vortex strengths is then repeated. This iteration procedure has proven to be computationally efficient. A complete description of this jet-flap analysis is given by Bevilaqua, Woan & Schum (1981).

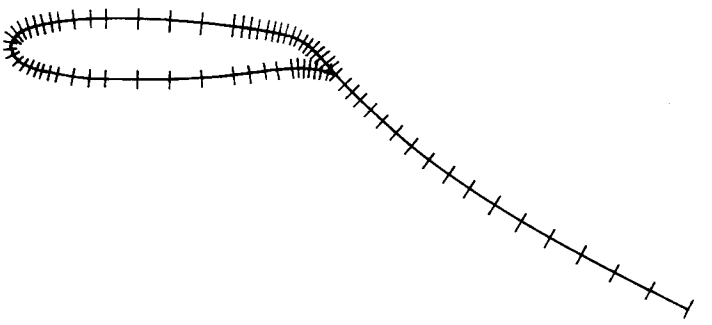

FIGURE 3. Distribution of curved panels on the airfoil and jet sheet.

3.3. *Matching procedure*

The inviscid solution for the airfoil drag is matched to the viscous solution for the jet thrust as follows. For given distributions of jet thrust and sink strength, the inviscid analysis yields an estimate of the jet shape. The curvature and streamwise pressure gradient along the jet then provide a set of boundary conditions for calculating the jet thrust and entrainment with the viscous analysis. These solutions are iterated until the computed reduction of jet thrust and the jet drag induced on the airfoil converge to within acceptable limits. The iterations are started with the simple case in which the jet thrust is assumed to be constant, and the sink strengths are all zero. Generally, three to four iterations are required to obtain convergence.

The curvature of the jet at each point along its length is determined by the local isentropic thrust T_*, which is defined to be the thrust obtained by an isentropic expansion (without additional mixing) of the local mass of the jet to the pressure at infinity. This is equal to the final thrust of the jet minus the thrust loss due to mixing downstream of the point. The local thrust of the jet is evaluated from the turbulent solution for the local jet velocity distribution in the following way. The local thrust is given by the expression

$$T_* = \dot{m}_j U_\infty + \rho \int_{-\infty}^{+\infty} U_*(U_* - U_\infty)\,\mathrm{d}y_*, \tag{12}$$

in which U_* prescribes the velocity distribution of the expanded jet and y_* is the transverse coordinate. Since the expansion is assumed to occur without mixing, the continuity equation for each stream tube yields

$$\rho U_*\,\mathrm{d}y_* = \rho U\,\mathrm{d}y. \tag{13}$$

Thus the local thrust can be written as

$$T_* = \dot{m}_j U_\infty + \rho \int_{-\infty}^{+\infty} U(U_* - U_\infty)\,\mathrm{d}y. \tag{14}$$

Then, since U_* is defined by Bernoulli's equation

$$\tfrac{1}{2}\rho U_*^2 + P_\infty \equiv \tfrac{1}{2}\rho U^2 + P, \tag{15}$$

the local thrust can be expressed in terms of the local jet-velocity distribution:

$$T_* = \dot{m}_j U_\infty + \rho \int_{-\infty}^{+\infty} U\left(\left[U^2 + \frac{2(P-P_\infty}{\rho}\right]^{\frac{1}{2}} - U_\infty\right)\mathrm{d}y. \tag{16}$$

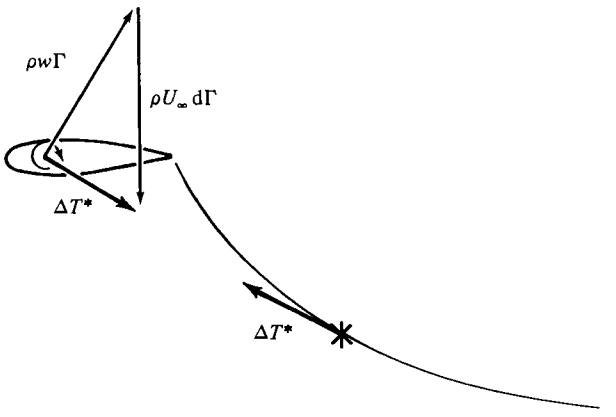

FIGURE 4. Equal and opposite jet drag forces induced on the airfoil and jet sheet.

In the irrotational flow on each side of the jet, $U = U_s$ and

$$\frac{2(P-P_\infty)}{\rho} = U_\infty^2 - U_s^2. \tag{17}$$

As a result, this integral differs from zero only within the jet, and the local thrust can be evaluated from the turbulent solution for the velocity profiles within the jet.

As a footnote to this discussion, Jones (see Schlichting 1979) suggested using T_* for evaluating airfoil drag from wake survey data. However, T_* varies in the streamwise direction as the jet drag reduces the wake momentum. Only in the far wake, where $\Delta P \ll \rho U^2$, does T_* equal the total drag. Thus, when Jones' method is used in the near wake, it does not yield the total drag (or thrust). The error is of the order of $\frac{1}{2}\Delta P^2 \delta$, where δ is the thickness of the jet or wake.

The force on a section of the jet and the equal but opposite reaction force on the airfoil are shown in figure 4. The force on the airfoil has two components: one due to a change in airfoil circulation $\rho U_\infty \, d\Gamma$; and another due to a change in the velocity at the airfoil $\rho w \Gamma$. The jet sink strengths are defined to produce this force on the airfoil. Thus they represent the change in the excess mass of the jet $\rho(U - U_s)\,\delta$, and not the mass actually entrained into the jet. This aspect of the model is important to understand. Since the jet is reduced to a thin sheet in the inviscid model, the actual spreading of the jet is not represented. Rather, it is the effect of the jet mixing which must be represented, and this effect is a force on the airfoil.

The sink strength at each point on the jet was therefore obtained by equating the horizontal component of the thrust loss to the horizontal force induced on an equivalent sink by all the other flow singularities,

$$\Delta T_* \cos\theta = \rho Q (U_T \cos\theta - U_\infty), \tag{18}$$

in which Q is the local sink strength, θ is the local jet deflection angle, and U_T is the tangential velocity on the jet streamline from the previous inviscid solution. In the next inviscid calculation, the airfoil circulation changes to include the effect of the sink. Therefore, when the iterations have converged, both components of the force are determined.

4. Experimental methods

4.1. *Experimental apparatus*

The wind tunnel used to measure the thrust recovery was designed to minimize blockage and ground interference effects during powered-lift testing. It is of the open-return type. Room air is drawn through a 4:1 contraction cone and the test section by a multitube ejector, which exhausts the flow back into the room. The ejector consists of 300 round nozzles, approximately $\frac{3}{16}$ in. in diameter. The test section is approximately 20 in. wide, 12 ft high, and 14 ft long. The vertical sides are diverged approximately 1.5 in. to compensate for wall-boundary-layer growth. The maximum tunnel speed was limited by the available air supply to about 100 ft/s.

The jet-flapped airfoil model was mounted approximately 5 ft from the end of the contraction and 7 ft from the floor. It had an 8 in. chord and spanned the test section. The airfoil was symmetric, except in the area of the jet-flap nozzle. This nozzle was located on the upper surface of the model at the hinge line of a 10 % chord flap. In order to assure that full leading-edge suction was obtained, the airfoil was 20 % thick and had a leading-edge radius equal to 5.5 % of the chord. Additional details regarding the tunnel and model are given by Bevilaqua *et al.* (1980).

4.2. *Instrumentation and procedures*

The boundary layer that develops on the tunnel sidewalls presents the major difficulty in obtaining two-dimensional airfoil data. The sectional lift of the airfoil is reduced within these boundary layers, and the resulting three-dimensionality of the lift distribution generates an induced drag. If the sidewall boundary layers separate in the adverse gradients due to the model, these problems are aggravated. Thus a pair of boundary-layer control jets were installed in each sidewall, upstream of the airfoil and at midchord, to prevent separation on the sidewalls.

There are also problems in measuring the forces on the model. If a balance is used, it is necessary to devise joints or end seals, and to make corrections for the non-uniform forces on the ends or corners. These problems are substantially more complicated on a jet-flapped model, since it is necessary to bridge the balance with the air supply for the jet. Various techniques have been devised to solve these problems, but each installation is unique and required considerable development.

In view of these complications, we decided to obtain the lift from airfoil surface pressure measurements, and the thrust from wake surveys. The surface pressures were also integrated to provide an alternative calculation of the thrust. To this end, the model was instrumented with a total of 82 static pressure taps. There were 74 taps arranged in a streamwise row on the airfoil and flap at midspan. A tap was located on the blunt base of the flap, and another was on the base of the nozzle lip. The other 8 taps were arranged in two spanwise rows to monitor the two-dimensionality of the pressure distribution. These taps were read by the same transducer using a scanivalve.

The jet wake was surveyed with a United Sensor type DC-125 three-dimensional flow probe. This Pitot-static probe has a conical head with one total pressure port and 4 separate static pressure ports. It was calibrated in an air jet of known direction to measure total and static pressures, as well as flow angularity, over a range of $\pm 50°$ in pitch, and $\pm 20°$ in yaw. Each of the 5 ports was read by a separate transducer.

Once the desired test conditions (airfoil angle of attack, jet-deflection angle, and jet-thrust coefficient) were set, data acquisition was controlled by computer. Model and tunnel operating conditions were first read, and then the scanivalve was cycled

for the surface pressure data. The computer then commanded the wake probe to traverse the jet for a specified number of data points and distance between points. Acquiring the data for each test condition required approximately 15 min.

The output signals from all instrumentation was reduced to engineering units on an IBM 1800 data acquisition computer, and the integration of the surface pressures for lift and drag, and the wake surveys for drag were then performed on an IBM 370 computer. The wake integration formula was derived by applying the momentum theorem to control surfaces ahead of and behind the model. If the upstream control surface is far enough away for the flow across it to be undisturbed, the momentum equation yields

$$T = \int_s (P+\rho U^2)\,\mathrm{d}y - \int_1 (P_\infty + \rho U_\infty^2)\,\mathrm{d}y, \tag{19}$$

in which 1 refers to the upstream surface and s refers to any downstream surface. By factoring and recombining the terms, we get

$$T = \rho \int_{-\infty}^{+\infty} U(U-U_\infty)\,\mathrm{d}y + \rho U_\infty \int_{-\infty}^{+\infty} (U-U_\infty)\,\mathrm{d}y + \int_{-\infty}^{+\infty} (P-P_\infty)\,\mathrm{d}y. \tag{20}$$

The continuity equation expresses the fact that the difference in mass flow between the upstream and downstream stations is equal to the mass added by the jet; that is,

$$\rho \int_{-\infty}^{+\infty} (U-U_\infty)\,\mathrm{d}y = \dot{m}_\mathrm{j}. \tag{21}$$

Substituting this relation into the momentum equation then yields the following expression for the net thrust on the airfoil

$$T = \dot{m}_\mathrm{j} U_\infty + \rho \int_{-\infty}^{+\infty} U(U-U_\infty)\,\mathrm{d}y + \int_{-\infty}^{+\infty} (P-P_\infty)\,\mathrm{d}y. \tag{22}$$

The first term is the source thrust generated by the added mass of the jet. The second term is the integral of the excess momentum; it represents the part of the initial jet momentum which is greater than the displaced freestream momentum. The last term represents the pressure force due to the deflection of the jet. It equals the difference between the horizontal component of the local jet thrust, and the thrust of the completely deflected jet. Since the jet approaches the freestream direction asymptotically, the total thrust can, in principle, be determined only from a survey at downstream infinity, or from a survey which extends to infinity above and below the jet. However, if the jet is nearly parallel to the freestream, the tangential component of the jet thrust is equal to the value recovered at infinity, within experimental error. Thus the measured tangential thrust was used to determine the thrust recovery. The integration of (22) was performed using the method of Betz, as described by Schlichting (1979).

4.3. *Thrust-recovery evaluation*

The thrust-recovery factor is defined to be the fraction of the total jet thrust that is actually recovered as a horizontal force on the airfoil; that is,

$$r = F_x/T. \tag{23}$$

In practice, the thrust loss is taken to be the increase in the profile drag of the unblown airfoil due to the entrainment drag and flow separation induced by the jet. Thus the viscous drag of the unblown airfoil is subtracted from the total drag of the blown

configuration. The thrust-recovery factor from the wake integration is therefore given by

$$r_{\mathrm{w}} = \frac{T_q + T_x + |D_{\mathrm{v}}|}{T}, \tag{24}$$

in which T_q is the source thrust, T_x is the excess momentum integral evaluated by the method of Betz, and D_{v} is the viscous drag of the unblown airfoil.

Since the flow would separate from the actual unblown airfoil at high lift coefficients, the viscous-drag correction was estimated by computing the skin friction drag and the pressure drag due to the boundary-layer displacement thickness. This is considered well within the capabilities of existing airfoil codes, but was verified by comparison with limited data for our geometry. The computed viscous-drag coefficient is described by the function

$$C_{D_{\mathrm{v}}} = 0.007 C_{\mathrm{L}}^2 + 0.022. \tag{25}$$

Variations in the lift coefficient C_{L} were obtained by changing the angle of attack. The actual airfoil coordinates and test Reynolds number were used for the drag computation.

The drag obtained by integrating the airfoil surface pressures also includes the pressure drag due to viscosity, but not the skin-friction drag. Thus, the pressure drag of the unblown airfoil is added to the measured surface pressure drag. In addition, however, an induced drag correction must be made because end effects introduce some three dimensionality in the surface-pressure distributions. The thrust recovery factor from the surface pressure integration is therefore given by

$$r_s = 1 - \left| \frac{D_s + D_p + D_{\mathrm{i}}}{T} \right|, \tag{26}$$

in which D_s is the integral of the surface pressures, D_p is the computed viscous pressure drag of the unblown airfoil, and D_{i} is the induced drag correction.

Foley (1962) estimated the induced drag by extrapolating the linear section of the drag polar of the unblown airfoil to the large lift coefficients of the jet-flapped airfoil. This is equivalent to assuming that the lift and jet thrust are elliptically distributed along the span. A similar approach was taken in this study, but the large values of the thrust coefficient considered here required using the expression for the induced drag of a jet-flapped wing devised by Maskel & Spence (1959),

$$C_{D_{\mathrm{i}}} = \frac{C_{\mathrm{L}}^2}{\pi A\, Re + 2C_\mu}. \tag{27}$$

In effect, Foley (1962) neglected the thrust-coefficient term C_μ, but over the range of values he examined ($C_\mu < 1$), the error is small. In this study, the effective aspect ratio of the airfoil was determined by subtracting the computed viscous drag from the measured total drag of the unblown airfoil. The total drag is described by the function

$$C_{\mathrm{D}} = 0.011 C_{\mathrm{L}}^2 + 0.022. \tag{28}$$

The effective aspect ratio of the airfoil is then obtained from the relation

$$A\, Re = \frac{C_{\mathrm{L}}^2}{\pi (C_{\mathrm{D}} - C_{D_{\mathrm{v}}})}. \tag{29}$$

This procedure gave $A\, Re = 77$, which was then assumed to be independent of variations in C_μ and θ_0.

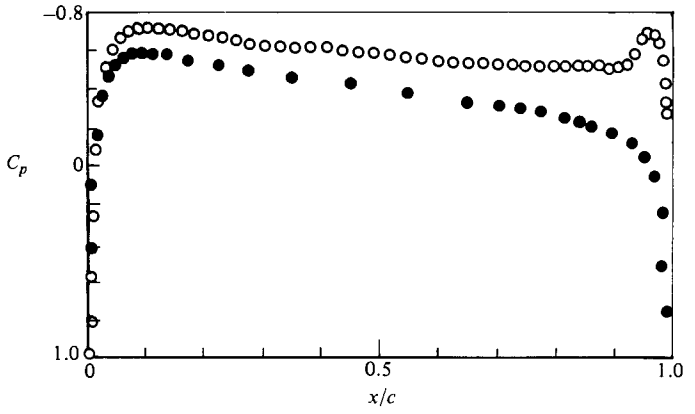

FIGURE 5. Airfoil surface pressure distributions: ●, without jet entrainment effect; ○, with jet entrainment effects.

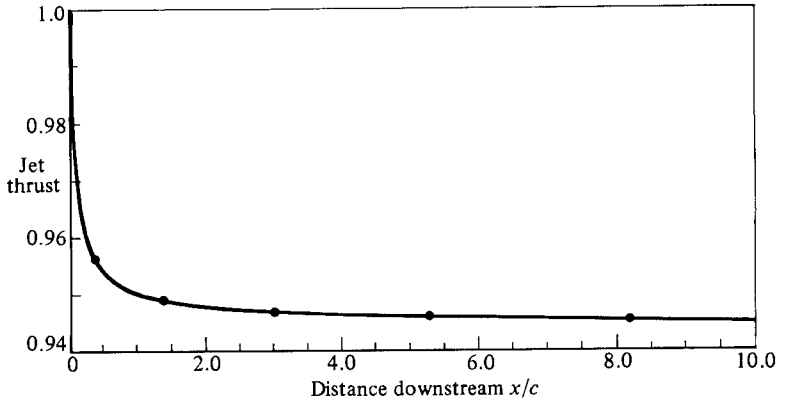

FIGURE 6. Streamwise variation of the local isentropic thrust of the jet.

5. Results and discussion

5.1. *Predicted thrust recovery*

As an example of the analytical results, the computed jet drag of the symmetrical airfoil is shown in figures 5 and 6. The jet was considered to originate at the rear stagnation point and trail straight back along the stagnation streamline. A Reynolds number of 300000 and jet-thrust coefficient of $C_\mu = 1$ were used, but it was assumed that the viscous drag of the airfoil was zero.

A total of three iterations were required for convergence. In figure 5 the computed surface pressure distribution for the airfoil and jet is compared with the computed distribution for the unblown airfoil. It can be seen that the effect of the jet is to accelerate the flow over the aft surface of the airfoil and thus induce a base drag. Integration of the surface pressures yields a pressure drag coefficient of $C_D = 0.050C_\mu$. The streamwise variation of the jet thrust is showm in figure 6. By $x/c = 7$ the thrust loss is $C_D = 0.051C_\mu$. Considering the difficulty in accurately integrating surface pressures, and the fact that T_* approaches the total thrust asymptotically, this is considered to be good agreement.

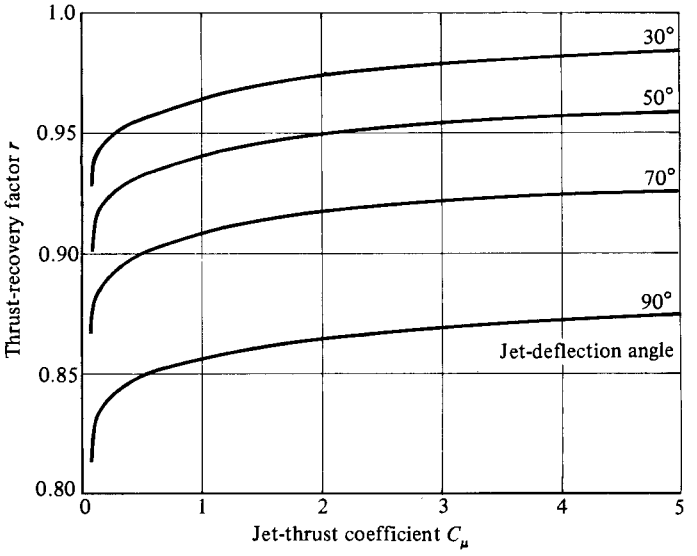

FIGURE 7. Predicted dependence of the jet-flap thrust recovery on the jet-thrust coefficient and initial deflection angle.

The calculated dependence of the jet-flap thrust recovery on the jet-thrust coefficient and deflection angle is shown in figure 7. The recovery factor decreases as the jet deflection angle increases, in agreement with Wygnanski's (1966) jet-drag hypothesis. However, the effect is small; even for 90° of deflection, the thrust loss is only about 15%. It is perhaps more surprising that the recovery factor increases as the thrust coefficient increases, rather than decreasing towards $\cos\theta$, which must be the limit as $C_\mu \to \infty$. This happens because the influence of the freestream dominates the pressure field for small values of C_μ. Thus the initial effect of increasing C_μ from zero is to accelerate the flow on the stagnation streamline at the airfoil's trailing edge. The adverse pressure gradient along the jet axis becomes less adverse and, as implied by (7), the thrust recovery improves. As C_μ gets larger, the freestream velocity becomes smaller than the velocity induced by the jet entrainment. Eventually, the effect of the freestream on the airfoil surface-pressure distribution vanishes, and the recovery factor approaches the correct limit. However, it will be seen that in real fluids the flow separates from the airfoil before this limit is attained.

5.2. *Measured thrust recovery*

The only previously available thrust-recovery data (Foley 1962; Quanbeck 1963) is for $C_\mu < 1$. Although the airfoil profile and test Reynolds numbers were not the same as in our study, the measured thrust recovery is on the same order as our calculated results. The thrust-recovery factors obtained in our study from both the surface-pressure and wake survey data are compared in figure 8. There is surprisingly good agreement between methods, although the surface-pressure data give consistently higher recovery. Based on our prior experience with wake and surface-pressure integrations, it is our feeling that the wake survey data are more reliable. However, the differences observed are within the 16% range of experimental error associated with previous measurements of thrust recovery (Leaman & Plotkin 1972).

In general, the measured thrust recovery decreases as the jet-thrust coefficient and initial deflection angle are increased. However, the variation is not continuous. For

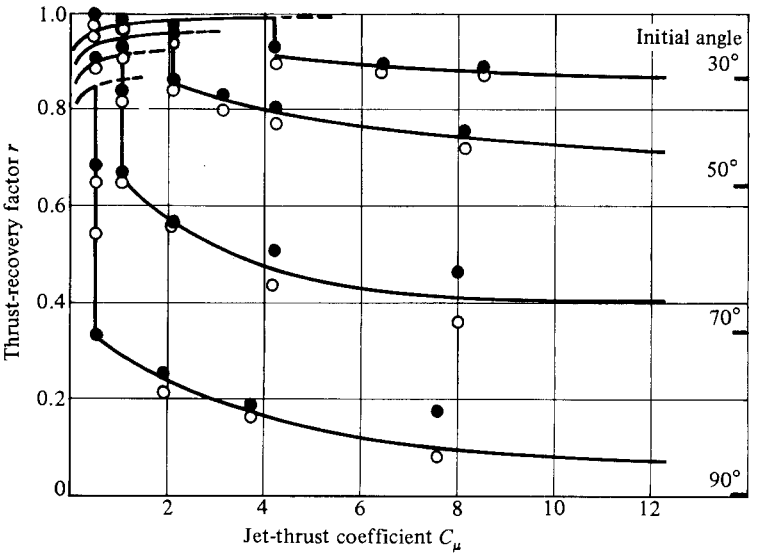

FIGURE 8. Measured variation of the jet-flap thrust recovery with the jet-thrust coefficient and initial deflection angle: ●, derived from surface-pressure integration; ○, derived from wake survey.

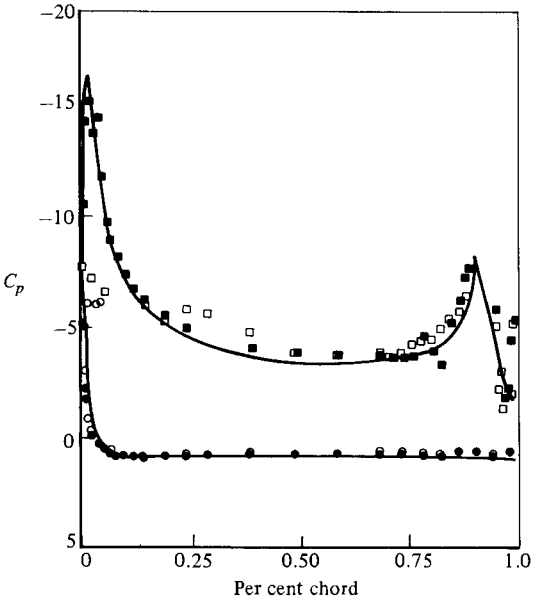

FIGURE 9. Measured surface-pressure distribution: ■, upper surface, attached flow; ●, lower surface, attached flow; □, upper surface, separated flow; ○, lower surface, separated flow.

every value of the deflection angle, there is a discontinuous change in the recovery for a value of the thrust coefficient of approximately $C_\mu = 2$. During the test, a distinct increase in noise level could be heard when the discontinuity occurred. Comparison of the measured airfoil surface-pressure distributions just before and after the discontinuity reveals that it is due to the bursting of the leading-edge separation bubble. This is shown in figure 9 for the $\theta_0 = 50°$ case. There is a change between

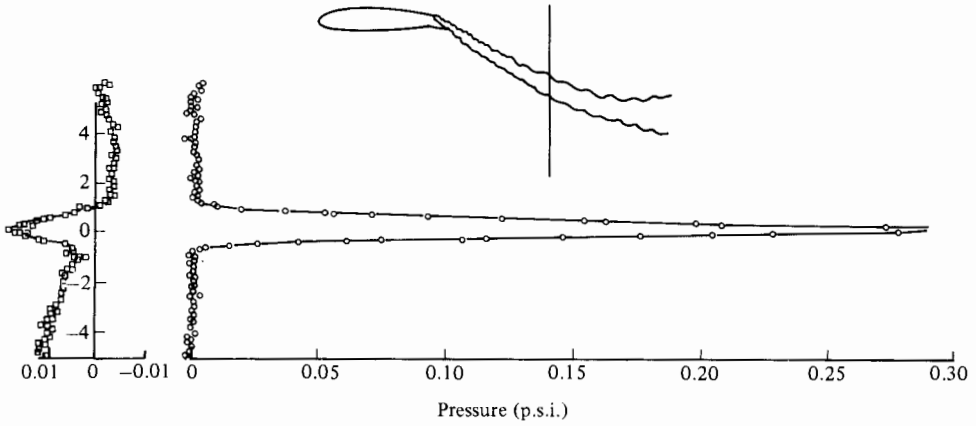

FIGURE 10. Representative wake survey data, $C_\mu = 1$, $\theta = 50°$: □, static pressures; ○, total pressures.

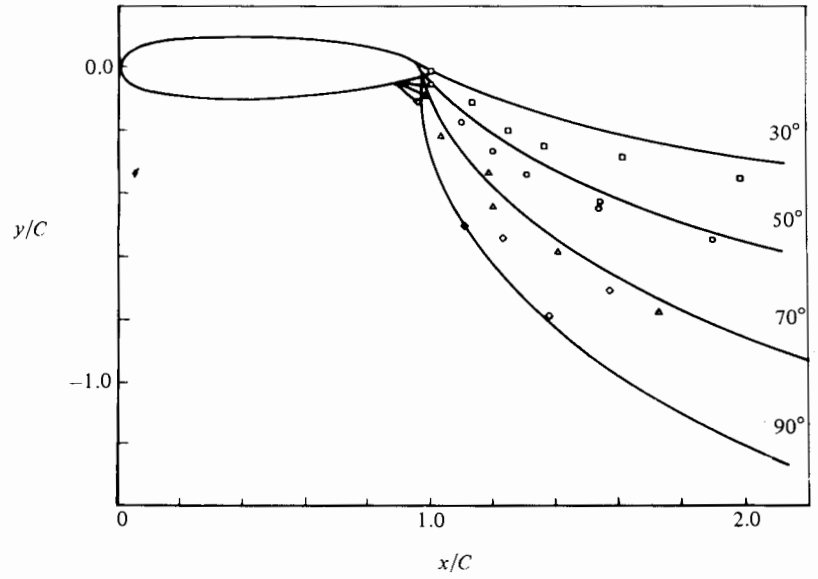

FIGURE 11. Effect of varying the initial jet-deflection angle: □, 30°; ○, 50°; △, 70°; ◇, 90°; ——, analytical predictions.

a short separation bubble, which gives larger recovery, and a long bubble which gives less recovery. Although the thrust recovery continues to decrease as the long bubble grows, there is no change when the bubble ultimately fails to reattach to the surface of the airfoil at all. Similar behaviour was reported by Dimmock (1957); however, there were 'so many sources of loss' that its significance has not been recognized.

The bursting of the bubble depends on the Reynolds number and Mach number of the flow, and the leading-edge radius of the airfoil, so that these results cannot be generally applied. However, the value of the thrust-recovery factor is reasonably well predicted by the jet-drag analysis up to the point of bursting. Thus it can be concluded that the loss of recovery up to the burst point is due to jet-entrainment drag, and that the short bubble does not significantly affect the thrust integrals.

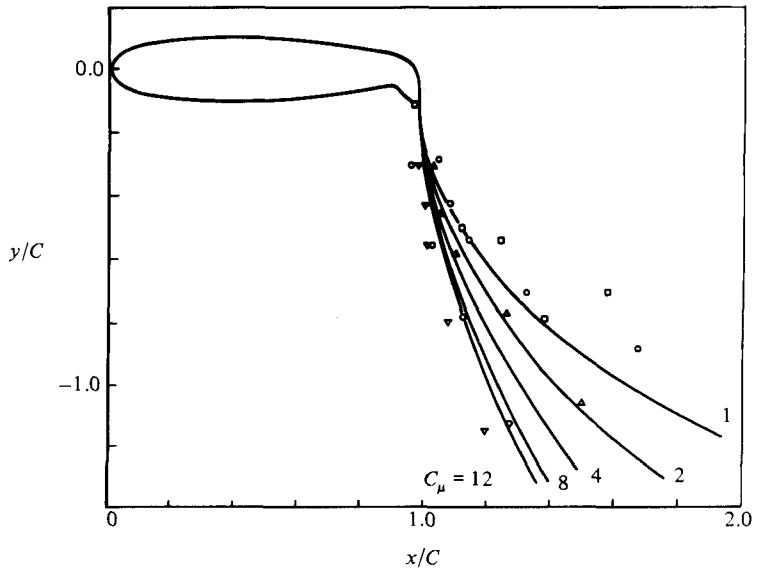

FIGURE 12. Effect of varying the jet-thrust coefficient: □, $C_\mu = 1$; ○, 2; △, 4; ●, 8; ▽, 12.

For small values of the jet-thrust coefficient, the thrust recovery actually increases slightly as the jet-deflection angle is increased from 0° to about 45°. Similar behaviour was seen in Foley's (1962) data, and in the calculated thrust recovery. Because the static pressure on the upper surface of the flap becomes more negative as the jet is deflected, there may actually be some thrust augmentation in this case. However, the effect is small and not sufficient to overcome the entrainment drag which occurs farther downstream.

5.3. *Jet wake characteristics*

A representative set of wake survey data for a case in which the flow did not separate from the airfoil is shown in figure 10. The total pressure profile has the familiar bell shape, and the static pressure is less above the jet than below it. This pressure jump is represented by the vortex sheet in Spence's (1956) theory. The reduction in static pressure within the jet is due to the jet turbulence, which causes an actual reduction in the pressure and introduces an error in the probe reading. Since the error is small, no correction was made. When the flow did separate from the airfoil, a region of low total pressure was seen above the jet.

The wake of every configuration was surveyed at the same station. But, in addition, some configurations were surveyed at several stations, in order to determine the jet development. In figure 11 the variation of the jet trajectory with the initial jet-deflection angle is shown for the case with $C_\mu = 1$. As might be expected, the penetration of the jet increases with the initial deflection angle. The effect of the jet momentum coefficient on the trajectory is shown in figure 12 for an initial deflection angle of 90°. As the blowing coefficient is increased, the jet tends to straighten out. In the limit as $C_\mu \to \infty$, the jet continues along the initial trajectory and the horizontal force on the airfoil becomes $T\cos\theta$. The complete set of surface pressure and wake survey data are contained in Bevilaqua *et al.* (1980).

The predictions of the jet trajectory given by the initial inviscid solution, in which complete thrust recovery is assumed, are shown for comparison in figures 11 and 12.

It can be seen that the inviscid theory provides a reasonable prediction of trajectory, even for cases in which there is a large separated wake.

6. Conclusions and recommendations

The mechanism of thrust recovery is an inviscid interaction between the airfoil circulation and the vorticity associated with the pressure jump across the jet. This interaction induces a pressure thrust on the airfoil and an equal but opposite force on the jet. If mixing is neglected, the jet becomes a streamline of the flow and is eventually turned in the direction of the freestream. This gives complete thrust recovery. Real-fluid effects reduce the actual recovery by causing airfoil boundary-layer separation, which reduces the pressure thrust, and by producing jet entrainment, which induces a base-pressure drag on the airfoil.

The thrust recovery is a function of both the thrust coefficient and the jet deflection angle. At small values of the thrust coefficient ($C_\mu < 1$), the jet mixing drag reduces the thrust recovery factor by about 10 %. As the jet thrust is increased, the recovery improves slightly, owing to changes in the local pressure gradient. However, for larger values of jet thrust, flow separation on the airfoil causes a loss of thrust recovery. At a fixed deflection angle, there is a discontinuous change in the recovery factor as the character of the separation changes from a 'short' bubble which reattaches to the airfoil near the leading edge, to a 'long' bubble which reattaches near the trailing edge. At higher values of C_μ, the bubble does not reattach to the airfoil at all, but is entrained into the jet wake. In general, it can be assumed that the thrust recovery is almost complete at small values of the jet thrust and deflection angle, but decreases to the horizontal component of the jet reaction force when the flow separates at larger values of these parameters.

A viscid/inviscid interaction analysis has been developed to compute the contribution of the jet drag to the reduction in thrust recovery. It was found that the entrainment drag accounts for the loss of recovery before bursting occurs. Thus such an analysis can be used to predict the thrust recovery of various jet-flap concepts, if the flow is prevented from separating by the use of slats, etc. In addition, the inviscid solution for the jet trajectory gives a good approximation to the measured trajectory, even for cases in which there is a large, separated wake.

Because flow separation plays such an important part in determining the thrust recovery at large values of the thrust coefficient, further development of jet-flap theory should focus on predicting the effects of separation.

The study was supported by the Air Force Office of Scientific Research under Contract F49620-78-C-0069.

REFERENCES

Bevilaqua, P. M., Cole, P. E. & Schum, E. F. 1980 Progress towards a theory of jet flap thrust recovery. *AFOSR Rep.* NR80H-76.

Bevilaqua, P. M., Woan, C. J. & Schum, E. F. 1981 Viscid/inviscid interaction analysis of ejector wings. *NASA* CR-166172.

Davidson, I. M. 1956 The jet flap. *J. R. Aero. Soc.* January 1956, 25–50.

Dimmock, N. A. 1957 Some early jet flap experiments. *Aero. Q.* November 1957, 331–345.

Foley, W. M. 1962 An experimental study of jet flap thrust recovery. PhD thesis, Stanford University; *SUDAER* 136.

HALSEY, N. D. 1974 Method for the design and analysis of jet-flapped airfoils. *J. Aircraft* **11**, 540–546.

HESS, J. L. 1973 Higher-order numerical solution of the integral equation for the two-dimensional Neumann problem. *Comp. Meth. in Appl. Mech. & Engng* **2**, 1–15.

HUNT, I. A. & JOUBERT, P. N. 1979 Effects of small streamline curvature on turbulent duct flow. *J. Fluid Mech.* **91**, 633–659.

LAUNDER, B. E. & SPALDING, D. B. 1972 *Mathematical Models of Turbulence.* Academic.

LEAMON, R. G. & PLOTKIN, A. 1971 An improved solution of the two-dimensional jet-flapped airfoil problem. *J. Aircraft* **9**, 631–635.

MCCORMICK, B. W. 1967 *Aerodynamics of V/STOL Flight.* Academic.

MASKELL, E. C. & SPENCE, D. A. 1959 Theory of the jet flap in three dimensions. *Proc. R. Soc. Lond.* A **251**, 407–425.

METRAL, A. & ZERNER, F. 1953 The Coanda effect. *Pub. Sci. et Tech. du Min. de l'Air* no. 218 (1948), *MOS*, TIB/T4027.

PATANKAR, S. V. & SPALDING, D. B. 1970 *Heat and Mass Transfer in Boundary Layers.* International Textbook Co., Ltd., London.

QUANBECK, A. H. 1963 Further verification of jet flap thrust recovery and identification of its mechanism. PhD thesis, Stanford University; *SUDAER* 144.

SCHLICHTING, H. 1979 *Boundary Layer Theory.* McGraw-Hill.

SPENCE, D. A. 1956 Lift coefficient of a thin, jet-flapped wing. *Proc. R. Soc. Lond.* A **238**, 46–68.

STRATFORD, B. S. 1956*a* Early thoughts on the jet flap. *Aero. Q.* February 1956, 45–59.

STRATFORD, B. S. 1956*b* Mixing and the jet flap. *Aero. Q.* May 1956, 85–105.

STRATFORD, B. S. 1956*c* A further discussion on mixing and the jet flap. *Aero. Q.* August 1956, 169–183.

TSONGAS, G. E. 1962 Verification and explanation of the controllability of jet flap thrust. Engineering thesis, Stanford University; *SUDAER* 138.

WILLIAMS, J., BUTLER, S. F. & WOOD, M. N. 1961 The aerodynamics of jet flaps. *ARC R & M* 3304.

WILSON, J. 1973 Thrust augmented wing sections in potential flow. PhD thesis, West Virginia University.

WYNGNANSKI, I. 1966 The effect of jet entrainment on loss of thrust for a two-dimensional symmetrical jet-flap aerofoil. *Aero. Q.* **17**, 31–52.